Tsuchiya and Thompson
Progress in Earth and Planetary Science (2022) 9:63
https://doi.org/10.1186/s40645-022-00521-3

Progress in Earth and Planetary Science

REVIEW

Open Access

The role of hydrogen bonds in hydrous minerals stable at lower mantle pressure conditions

Jun Tsuchiya[1*] and Elizabeth C. Thompson[2]

Abstract

Over the past few decades, hydrous minerals were thought to be absent in the lower mantle, due to their instability at high-pressure conditions. Recently, however, hydrous phases including phase H ($MgSiO_4H_2$), pyrite-type FeOOH, and δ-AlOOH have been discovered to be thermodynamically stable at lower mantle pressures. Investigations using ab initio calculations methods play a key role in identifying these novel phases and determining their geophysical properties (i.e., compressibility, elasticity, and sound velocities). These calculations suggest that the hydrous minerals which are stable at lower mantle pressure conditions (i.e., phase H, FeOOH, and AlOOH), have symmetric hydrogen bonds at these pressures. This indicates that hydrogen bond strength is closely connected to the stability and physical properties of hydrous minerals at extreme pressures. In this review, we summarize the theoretical and experimental studies of hydrous minerals stable at the high-pressure conditions of the Earth's lower mantle in light of the role of hydrogen bonding.

Keywords: Hydrous minerals, Ab initio calculation, Hydrogen bond, High pressure, Lower mantle

1 Introduction

1.1 Water transport into the Earth's deep interior and the role of hydrous minerals

Water contained within minerals and rocks is thought to profoundly influence mantle dynamics on Earth, as the presence of water can significantly affect physical properties including the melting temperature, rheology, phase stability, and elasticity of Earth's constituent minerals (e.g., Hirschmann 2006). Determining the states and amount of water in the Earth's interior is therefore essential to understanding Earth's evolutionary processes, but the total water budget in the Earth's interior is largely unknown. Based on the proton accommodation capacity of nominally anhydrous minerals (NAMs) stable in the mantle transition zone, it has been suggested that the quantity of water (or more precisely, hydrogen and hydroxyl) stored in the mantle is equal to or greater than all of the water contained in all of Earth's surface reservoirs combined (a unit sometimes referred to as an Earth ocean) (e.g., Smyth 1994; Hirschmann and Kohlstedt 2012; Pearson et al. 2014). In order to discuss whether Earth's mantle is wet or dry, we must understand the fluxes of water into and out of the Earth's deep interior.

Hydrous minerals form by the reaction of magma and rocks with water at the Earth's surface. These minerals usually contain OH dipoles in the crystal lattice. In many cases, H_2O molecules are not included in the crystal structure of hydrous minerals and the chemical formula does not contain "H_2O," but H_2O is released during decomposition. For example, in the case of brucite, $Mg(OH)_2 \leftrightarrow H_2O+MgO$. Hydrous minerals such as phyllosilicates (serpentine, mica, clay, etc.) within subducting oceanic slabs transport water from the Earth's surface into the Earth's interior (Fig. 1). Phyllosilicates have layered crystal structures, with

*Correspondence: tsuchiya.jun.my@ehime-u.ac.jp

[1] Geodynamics Research Center, Ehime University, 2-5 Bunkyo-cho, Matsuyama, Ehime 790-8577, Japan
Full list of author information is available at the end of the article

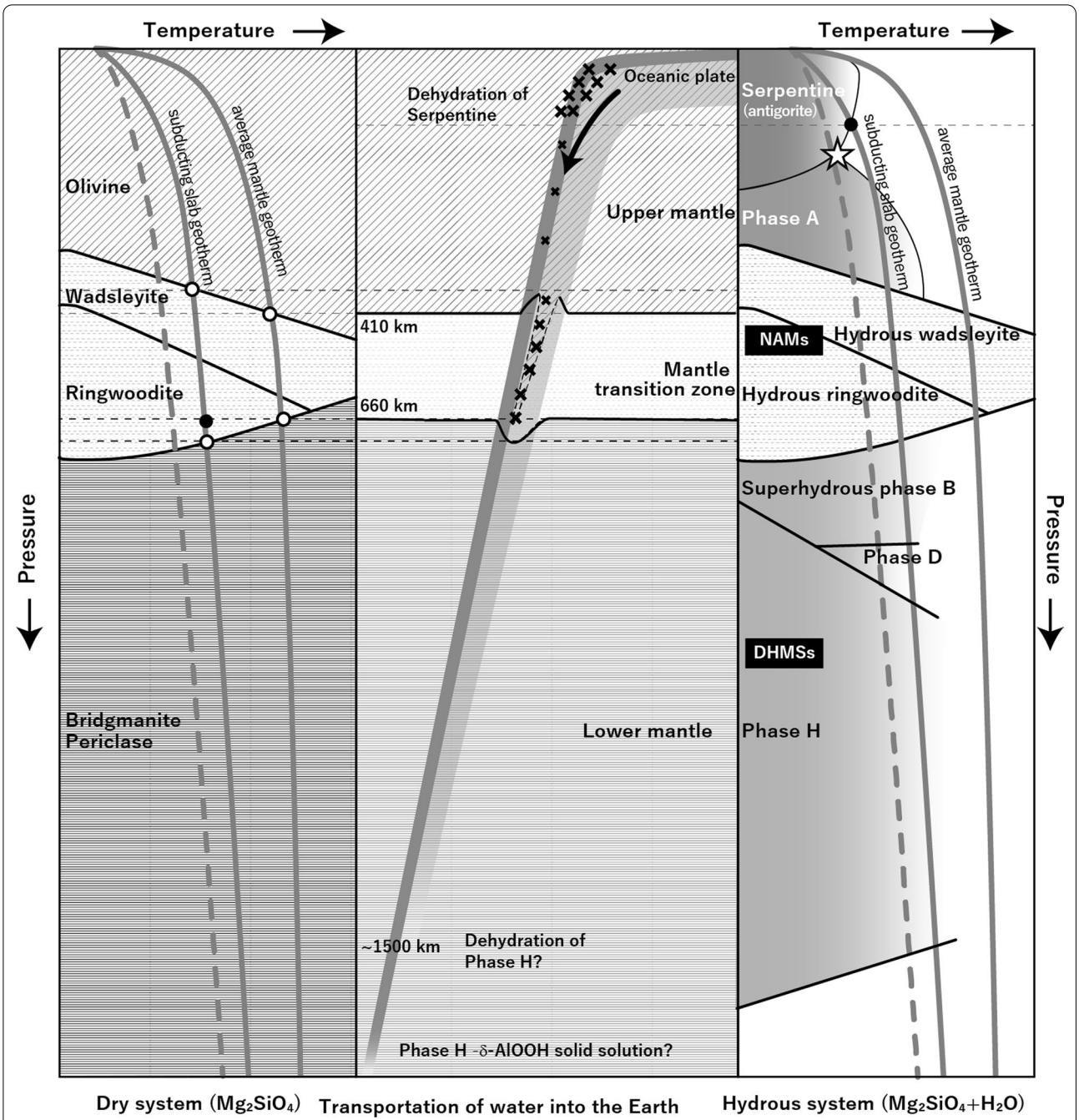

Fig. 1 Schematic illustration of the subducting slab (middle) and phase diagram of dry Mg_2SiO_4 (left) and "stability diagram" of wet systems (right). More detailed stability diagrams of hydrous phases are given in Ohtani et al. (2001b); Nishi et al. (2014); Ohtani (2020). The cross symbols indicate the seismicity observed in the subducting oceanic plate. The "choke point" is shown as the star symbol. Below the choke point temperature, hydrous mineral can transport water into the deeper part of the Earth's interior

hydrogen bonds connecting the layers. Because hydrogen bonds are weaker (binding energy: 2–50 kJ/mol) than normal chemical bonds (e.g., ionic bonds: >600 kJ/mol, covalent bonds: 50–800 kJ/mol), hydrous minerals generally have lower densities and lower melting temperatures than anhydrous minerals. Furthermore, crustal (i.e., low pressure) hydrous minerals such as phyllosilicates generally dehydrate at high-pressure and -temperature conditions. Therefore, within the Earth's interior, hydrous minerals are typically found

in lower-temperature regions, such as cold, subducting oceanic slabs.

Initially, it was believed that the deep mantle was essentially dry because the hydrous minerals known at that time would typically decompose and release water at the high temperature and pressure conditions consistent with depths in the Earth of approximately 150 km (~5 GPa, 600 °C) (Fig. 1). More recently, however, a series of hydrous minerals have been discovered which are stable at higher pressure conditions, some of which can retain water even under the pressure conditions in the lower mantle. Currently, the high-pressure behavior and stability of hydrous minerals such as dense hydrous magnesium silicates (DHMSs) (Ringwood and Major 1967), which include phase A ($Mg_7Si_2O_8(OH)_6$), superhydrous phase B ($Mg_{10}Si_3O_{14}(OH)_4$), phase D ($MgSi_2O_4(OH)_2$), and phase H ($MgSiO_2(OH)_2$), are being vigorously investigated to clarify the role these phases play in the water cycle of Earth's deep interior (Fig. 1).

Subducting oceanic plates consist of sedimentary, basalt (mid-ocean ridge basalt, or MORB), and peridotite layers (Fig. 2). Each layer is a chemically distinct mineral assemblage consisting of different hydrous minerals (Table 1), therefore, the stability limit of these hydrous minerals is different in each of these layers. If a hydrous mineral in the peridotite layer decomposes at high-pressure conditions, then the released water can move upward due to its reduced density compared with the surrounding mantle. Here, water could form new hydrous minerals in the overlying basaltic and sedimentary rock layers. Conversely, the transition zone water filter theory of Bercovici et al. (2003) hypothesized that negatively buoyant hydrous melts generated above the transition zone might sink back into the transition zone and re-hydrate it. Either way, water released during decomposition and dehydration reactions have the opportunity to form new hydrous phases. For example, phase H ($MgSiO_4H_2$) decomposes at ~1500 km depth (60 GPa) in the pure Mg–Si system (i.e., the endmember composition with no Fe or Al in the system) (Nishi et al. 2018; Tsuchiya and Umemoto 2019). The water released by this reaction can then react to form another hydrous phase such as δ-AlOOH or solid solutions of δ-AlOOH and phase H [$(Mg,Al)(Si,Al)O_4H_2$] in the sedimentary rock layer. These newly formed hydrous phases could continue to be transported deeper into the mantle, as δ-AlOOH is stable to the pressure and temperature conditions of the base of the lower mantle (Sano et al. 2008a; Ohira et al. 2014).

1.2 Role of ab initio calculation for investigating Earth's interior

Since the deep interior of the Earth cannot be directly observed, our understanding of this region relies on a combination of seismic observations, high-pressure experiments on rocks and minerals, and theoretical calculations. Because hydrogen is the lightest element and has only one electron, it is difficult to detect at the

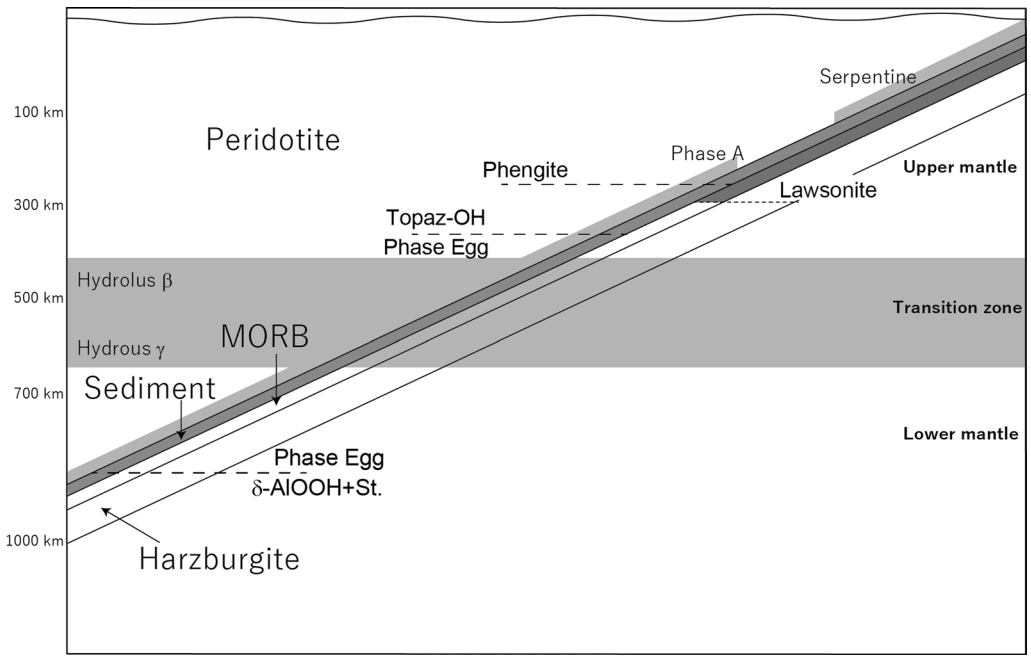

Fig. 2 Schematic illustration of water transport by the subducting slab. Gray areas represent wet regions (Modified from Ono (1998))

Table 1 Hydrous minerals, dense hydrous magnesium silicates (DHMSs), and nominally anhydrous minerals (NAMs) which could potentially exist in subducting oceanic plates Schmidt and Poli (1998); Inoue (2000); Ono (1998); Ohtani et al. (2001b). All Mg atoms can be replaced with Fe atoms in the chemical formula shown below

Mineral	Abbreviation	Formula
Hydrous peridotite		
Lizardite	Liz	$Mg_3Si_2O_5(OH)_4$
Antigorite	Atg	$Mg_{3m-3}Si_{2m}O_{5m}(OH)_{4m-6}$ (m=13~24)
Chlorite	Chl	$Mg_{12}(Si,Al)_8O_{20}(OH)_{16}$
Talc	Tlc	$Mg_3Si_4O_{10}(OH)_2$
Phase A	A	$Mg_7Si_2O_8(OH)_6$
Phase B	B	$Mg_{12}Si_4O_{19}(OH)_2$
Phase E	E	$Mg_{2.3}Si_{1.25}O_6H_{2.4}$
Superhydrous phase B (=Phase C)	SuB	$Mg_{10}Si_3O_{18}H_4$
Phase D (=Phase F=Phase G)	D	$MgSi_2O_6H_2$
Phase H	H	$MgSiO_4H_2$
Hydrous wadsleyite	β	Mg_2SiO_4 (H_2O<3.3 wt%)
Hydrous ringwoodite	γ	Mg_2SiO_4 (H_2O<2.7 wt%)
Hydrous MORB		
Amphibole	Amp	$Ca_2Mg_3Al_2Si_6Al_2O_{22}(OH)_2$
Lawsonite	Law	$CaAl_2Si_2O_7(OH)_2{\cdot}H_2O$
Sediment		
Phengite	Phe	$K(Al,Mg)_2(OH)_2(SiAl)_4O_{10}$
Topaz-OH	–	$Al_2SiO_4(OH)_2$
Phase Egg	Egg	$AlSiO_3OH$
δ-AlOOH	–	AlOOH
Pyrite-type AlOOH/γ-AlOOH		AlOOH
Goethite (α-FeOOH)	Goe	FeOOH
ϵ-FeOOH	–	FeOOH
Pyrite-type $FeOOH_x$	–	FeO_2H_x, x=0.39-1
HH phase	–	$(Fe,Al)O_2H_x$ (x~1?)

extreme pressure and temperature conditions relevant to the lower mantle using conventional experimental techniques such as X-ray diffraction or neutron diffraction. In X-ray diffraction, the small scattering cross section makes hydrogen difficult to detect, whereas neutron diffraction experiments require large sample volumes and are limited in their pressure range. In recent years, ab initio methods have become an important research tool in the field of deep Earth science, as these calculations complement and inform high-pressure experimentation and aide our investigation into the behavior of hydrogen and hydrogen bonds in deep Earth phases.

Ab initio calculation methods are used to elucidate phase relationships of minerals under ultra-high pressures that are difficult to access experimentally, to search for structures, and to determine physical properties including compressibility, elastic properties, seismic wave velocity, viscosity, optical properties, thermal conductivity, etc. It has also become possible to determine the thermodynamic properties and high-temperature and high-pressure phase diagram of minerals using ab initio free energy calculation methods (e.g., Giannozzi et al. 2009; Baroni et al. 2001; Tsuchiya et al. 2005b). Beyond probing the physical properties of known minerals, ab initio methods have been integral to the discovery of new phases by theoretically predicting their formation and providing the necessary temperature and pressure conditions to verify their stability experimentally. Ab initio calculations contribute to our understanding of the materials in the Earth's interior by providing insights into the physical and chemical characteristics of hydrous minerals with complex crystal structures and chemical bonds.

2 Review

2.1 Purpose of this review

In the past decade, our knowledge regarding hydrous minerals that are stable at the pressure and temperature conditions of the lower mantle (phase D, phase H, superaluminous phase D, δ-AlOOH, ϵ-FeOOH, pyrite-FeOOH, etc.) has grown at a remarkable pace (Pamato et al. 2014; Nishi et al. 2014, 2017, 2020; Thompson et al. 2021, 2022; Tsuchiya et al. 2002, 2005a; Verma et al. 2018). Constraining the stability and properties of these hydrous minerals is critical for understanding how water is stored and cycled in the Earth's deep interior. Interestingly, these high-pressure hydrous minerals also share a high likelihood of pressure-induced hydrogen bond symmetrization at the pressures of the lower mantle where they may be stable. Symmetric hydrogen bonding is a special type of hydrogen bond where hydrogen is equally covalently bonded to two adjacent anions (Fig. 3, part 5). Therefore, the increased strength of hydrogen bonding is presumably closely connected to the stability of these hydrous phases. In this review, we summarize the crystal structures and physical properties of these high-pressure hydrous minerals in terms of the role of hydrogen bonds, including the characteristics of the hydrogen bonds in each phase, as well as the possible existence of further high-pressure hydrous phases.

2.2 DHMSs in Earth's lower mantle

As described in the introduction, hydrous minerals in subducting oceanic plates with peridotite or peridotitic composition can react to form dense hydrous magnesium silicate phases (DHMSs) under pressure. Since the initial work of Ringwood and Major (1967),

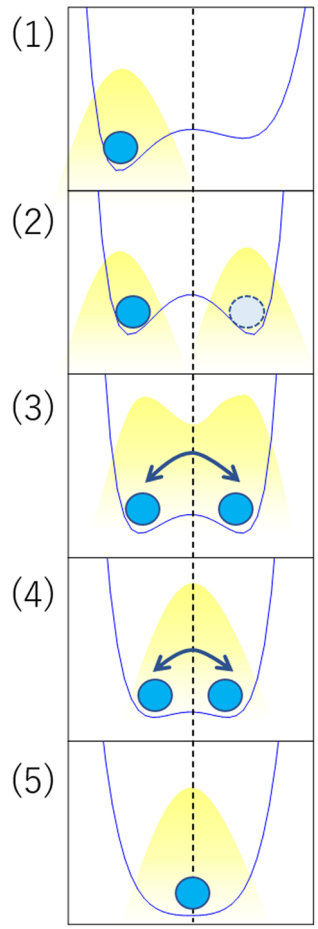

Fig. 3 Schematic illustration of proton distributions of the hydrogen bond in ice VIII/VII/X under pressure. (1) asymmetric hydrogen bond, (2) static disordering, hydrogen resides at one of double potential wells, (3) dynamical disordering with bimodal probability of proton (e.g., dynamically disordered ice VII) (4) dynamical disordering state with unimodal probability of proton at the midpoint of two oxygen atoms (dynamically disordered ice X), (5) symmetric hydrogen bond (ice X)

several DHMSs have been synthesized and reported by high-pressure experiments. Due to their stability in subducting slab compositions at pressure-temperature conditions consistent with cold slab subduction, DHMSs are thought to play a key role in transporting water to the Earth's deep interior (Table 1).

Two decades ago, a study using in situ X-ray diffraction found that phase D (ideal formula: $MgSi_2O_4(OH)_2$) either decomposes into anhydrous minerals and water at ~40 GPa or undergoes a phase transition to an unknown phase (Shieh et al. 2000). Based on this finding, it was believed that the transportation of water into the deep Earth via DHMSs terminated at the middle depth of the lower mantle (~1250 km in depth) (e.g., Albarede 2009). More recently, Tsuchiya (2013) suggested that phase D could react to form a newly recognized DHMS with the chemical composition of ($MgSiO_2(OH)_2$) above 40 GPa. Using ab initio calculations, Tsuchiya (2013) showed that the combined free energy of this new hydrous mineral ($MgSiO_2(OH)_2$) plus stishovite (SiO_2) was lower than that of phase D ($MgSi_2O_4(OH)_2$) above approximately 40 GPa, supporting their relative stability at higher pressures. Based on this theoretical prediction, high-pressure experiments using a multi-anvil high-pressure apparatus and in situ synchrotron X-ray diffraction were conducted to search for this new high-pressure DHMS (Nishi et al. 2014). These experiments confirmed that phase D undergoes a reaction to form a new high-pressure hydrous mineral with the predicted composition ($MgSiO_4H_2$) at the theoretically predicted pressure. This novel hydrous phase, which was named phase H, was the first new DHMS to be identified almost 30 years after the discovery of phase D in 1986 (Liu 1986).

The phase boundary between the phase D and the phase H + stishovite (SiO_2) has a positive Clapeyron slope (dP/dT=~6.4 MPa/K at 1000 K) (Tsuchiya 2013). In other words, phase H is stable at pressures above about 48 GPa at the temperature conditions of a subducting cold slab (i.e., about 500 K cooler than the mantle geotherm). The dissociation phase boundary of phase H in the lower mantle has been reported by calculating the Gibbs free energy of ice VII and $MgSiO_3$-bridgmanite (Tsuchiya and Umemoto 2019). That study indicates that phase H decomposes to $MgSiO_3$-Bridgmanite and H_2O at about 60 GPa and 1000 K. This estimation is also supported by the high-pressure experiments (Ohtani et al. 2014; Nishi et al. 2018). This finding indicates that phase H has the highest pressure stability among DHMSs, since it decomposes into anhydrous minerals and water above ~60 GPa. This means that the transportation of water by the sequential formation of Mg-endmember DHMSs is terminated by the middle of the lower mantle (60 GPa, depth of ~1500 km).

In reality, the mantle is a complex system containing several weight percentages of Al and Fe in addition to magnesium silicate minerals. Furthermore, high-pressure experiments show that in the Al-bearing system, Al selectively partitions into phase H rather than coexisting mantle minerals such as bridgmanite and ferropericlase, extending the stability of Al-bearing phase H toward higher pressure and temperature conditions (Nishi et al. 2014; Ohira et al. 2014). This Al-enriched phase can be tentatively regarded as a solid solution between phase H and δ-AlOOH, as they share the same crystallographic framework. Since the initial discovery of δ-AlOOH, it has been noted that this phase contained non-negligible

amount of Mg and Si (Suzuki et al. 2000). Although the phase relation between phase H and δ-AlOOH is still unknown, calculations support that phase H and δ -AlOOH form a complete solid solution (Panero and Caracas 2017). Endmember δ-AlOOH is stable over a very wide temperature and pressure range (33–134 GPa, 1350–2300 K) (Sano et al. 2008a). Therefore, the pressure-temperature stability of phase H is likely enhanced by the presence of Al, such that water may be transported to the core–mantle boundary (CMB) (Fig. 1).

2.3 High-pressure phase transitions of δ-AlOOH

δ-AlOOH is stabilized by a phase transition from diaspore (α-AlOOH) above 18 GPa. δ-AlOOH itself undergoes pressure-induced hydrogen bond symmetrization above 18 GPa (Sano-Furukawa et al. 2018). Therefore, δ -AlOOH retains the symmetric hydrogen bond within its thermodynamically stable conditions. This phase is known to have a wide thermodynamic stability field that extends to pressure and temperature conditions of up to 134 GPa and 2300 K (Sano et al. 2008a). It was theoretically predicted to undergo a phase transition to a pyrite-type structure (space group $Pa\bar{3}$) above 170 GPa (Tsuchiya and Tsuchiya 2011), with more recent work placing this transition closer to 190 GPa (Thompson et al. 2021). In order to confirm the phase transition to the pyrite-type AlOOH phase theoretically predicted, high-pressure experiments using diamond anvil cells (DACs) were conducted (Nishi et al. 2020). In that experiment, the transition from δ-AlOOH to new crystal structure with the orthorhombic symmetry (Space group *Pbca*) was detected at ~190 GPa. The crystal structure of this new phase had been predicted by ab initio calculation using an evolutionary genetic algorithm method (Verma et al. 2018) (Table 2). These calculations also indicate that the *Pbca* phase has a narrow stability field (166–189 GPa) and subsequently transforms to the pyrite-type structure at higher pressures. To date, however, the formation of pyrite-type AlOOH phase has not been confirmed by experiments even at the pressure-temperature conditions at which its stability was predicted by ab initio calculations. Further high-pressure, high-temperature

Table 2 The crystal structures of MOOH (M=Al, Fe, etc.)

Space group	Mineral name/phase	M coordination no.	References
AlOOH			
Pbnm	Diaspore α	6	Busing and Levy (1958)
Cmcm, etc.	Boehmite/γ		Corbato et al. (1985)
$P2_1nm$/Pnnm	δ	6	Suzuki et al. (2000)
Pbca	ϵ	6	Verma et al. (2018)
			Nishi et al. (2020)
$Pa\bar{3}$	Pyrite-type	6	Tsuchiya and Tsuchiya (2011)
FeOOH			
Pbnm	Goethite/α	6	Sampson (1969)
Cmcm	Lepidocrocite/γ	6	Oosterhout (1960)
$P2_1nm$/Pnnm	ϵ	6	Pernet et al. (1975)
$Pa\bar{3}$	Pyrite-type FeO_2H	6	Nishi et al. (2017)
	FeO_2H_x, 0.39<x<0,81		Hu et al. (2017)
InOOH			
Pnnm	-	6	Lehmann et al. (1970)
Pbca	-	6	Verma et al. (2018)
$Pa\bar{3}$	Pyrite-type	6	Sano et al. (2008b)
			Tsuchiya et al. (2008)
$P\bar{4}2_1m$	YbOOH-type	7	Verma et al. (2018)
			Christensen and Hazell (1972)
CrOOH			
$R\bar{3}m$	Grimaldiite/α	6	Christensen et al. (1977)
Pbnm	Bracewellite	6	Milton et al. (1976)
Pnnm	Guyanaite/β	6	Christensen et al. (1976)
MnOOH			
Pbnm	Groutite/α	6	Glasser and Ingram (1968)
$P2_1nm$/Pnnm	Manganite/γ	6	Kohler et al. (1997)

experiments are needed to determine if this discrepancy between theory and experiments is due to transition kinetics. Finally, above 300 GPa, the dissociation from pyrite-type AlOOH to $CaIrO_3$-type Al_2O_3 (Tsuchiya et al. 2005b) and ice X has been proposed based on calculations (Tsuchiya and Tsuchiya 2011).

δ-AlOOH has a crystal structure similar to that of the $CaCl_2$-type structure. As mentioned above, the solid solution of δ-AlOOH and phase H is considered to have a very wide thermodynamic stability region. However, their densities are small compared to the mantle constituent minerals, and their gravitational stability is questionable for the transport of water to the deep interior of the Earth. Therefore, it is necessary to investigate the influence of Fe, which is an important element in the mantle, on the thermodynamic and gravitational stability of δ-AlOOH and phase H.

2.4 High-pressure phase transitions of ϵ-FeOOH

At moderate pressures (>6 GPa), the mineral goethite (α-FeOOH) which is found in subducting slabs, transitions to the polymorph ϵ-FeOOH, which is isostructural with δ-AlOOH. Like δ-AlOOH, ϵ-FeOOH undergoes pressure-induced hydrogen bond symmetrization which produces the same $P2_1nm$ to $Pnnm$ phase transition (Xu et al. 2013; Gleason et al. 2013; Thompson et al. 2017, 2020). Additionally, experiments using X-ray emission spectroscopy (XES), X-ray diffraction, and optical absorption spectroscopy (Gleason et al. 2013; Thompson et al. 2020) reveal that the iron atoms in ϵ-FeOOH undergo a high-spin state to a low-spin state transition at ~45 GPa that produces a unit cell volume reduction of more than 10%. The isostructural nature of δ-AlOOH and ϵ-FeOOH make it possible for intermediate δ-(Al,Fe)OOH compositions to exist, and aluminum substitution is expected to increase the thermodynamic stability of the Al-rich compositions compared to the Fe-endmember (Xu et al. 2019). Research into the geophysical properties of intermediate δ-(Al,Fe)OOH, and their possible contribution to heterogeneity in the deep Earth is an active area of ongoing research (Ohira et al. 2019, 2021; Kawazoe et al. 2017; Satta et al. 2021; Suzuki et al. 2021; Buchen et al. 2021).

Based on the prediction that ϵ-FeOOH was likely to transition to the pyrite structure at high pressures analogous to the δ-AlOOH to pyrite-type AlOOH transition, the high-pressure phase diagram of FeOOH was determined using ab initio calculations (Nishi et al. 2017; Thompson et al. 2017). Ab initio density functional calculations using internally consistent U calculation (Cococcioni and de Gironcoli 2005) showed that the pyrite-type, low-spin FeOOH structure is stabilized at about 70 GPa. Simultaneously, high-pressure experiments using diamond anvil cells (DACs) revealed a phase transition to pyrite-type FeOOH at about 80 GPa (Nishi et al. 2017). Pyrite-type FeOOH is stable even under average mantle geotherm conditions (~95 GPa and 2400 K), and is significantly denser than both phase H and δ-AlOOH. Endmember pyrite-type FeOOH would sink toward the core–mantle boundary (CMB) owing to its notably higher density (6.939 g/cm^3 at 101 GPa) in comparison to the surrounding mantle. It has also been reported that ϵ-FeOOH undergoes a phase transition to the pyrite-type $FeOOH_x$ ($0.39<x<0.81$) where dehydrogenation partly occurs (Hu et al. 2017). It was argued that this reaction is important because it has a significant effect on the redox conditions in the deep Earth. Further studies are needed to confirm the effects of the dehydrogenation of FeOOH at the CMB. As with their respective lower-pressure polymorphs, the formation of intermediate (Al,Fe)OOH compositions in the pyrite-type structure, and research into the stability and geophysical properties of these intermediate compositions, is an area of particular interest to the deep Earth community (Nishi et al. 2020; Thompson et al. 2021).

2.5 Other MOOH structures

InOOH has a $CaCl_2$-type crystal structure at ambient conditions. The high-pressure phase transition of this type of structure is reminiscent of the high-pressure phase transition of SiO_2. The pyrite-type structure is stable above 250 GPa and 90 GPa in anhydrous SiO_2 and GeO_2, respectively (Ono et al. 2003; Kuwayama et al. 2005). The transition from the $CaCl_2$-type to the pyrite-type structure was first reported in InOOH by ab initio calculations and high-pressure experiments at 15 GPa (Sano et al. 2008a; Tsuchiya et al. 2008). In SiO_2, α-PbO_2-type structure (seifertite) exists as an intermediate phase between $CaCl_2$-type and pyrite-type, but this structure does not seem to be stabilized in MOOH compositions (M=Al, Ga, In) (Tsuchiya and Tsuchiya 2011).

GaOOH and InOOH can be used as the low-pressure analog materials of AlOOH, such that the higher pressure polymorph structure that follows pyrite-type InOOH and GaOOH would be a likely candidate for the higher pressure polymorph structure that follows pyrite-type AlOOH. Identifying and studying the higher pressure polymorph of AlOOH is important for investigating hydrogen cycling in the deep interiors of larger planets such as super-Earths and ice giants (Nishi et al. 2020). Using the GaOOH and InOOH systems allows us to search for this structure without necessitating the extreme conditions as would be needed to produce this phase transition in AlOOH. The high-pressure phases of MOOH (M=Al, Ga, In) compositions have been investigated by ab initio calculation combined with an evolutionary genetic algorithm method Verma et al.

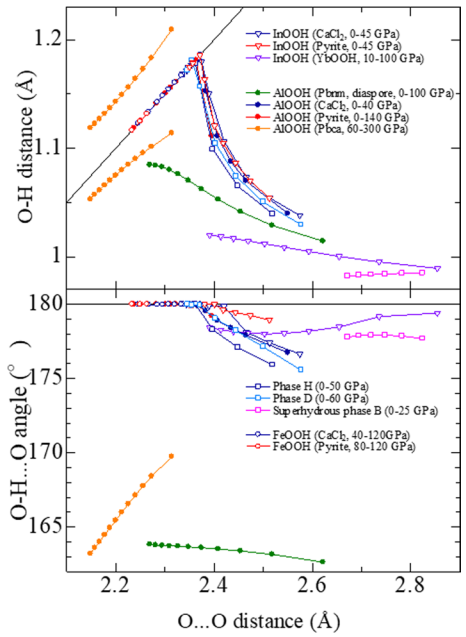

Fig. 4 The relationship between O· · ·O and O–H distances (upper panel), and O· · ·O distance and O– H...O angle (lower panel) of InOOH, AlOOH, FeOOH and DHMSs (Tsuchiya et al. 2002, 2005a; Tsuchiya 2013; Mookherjee and Tsuchiya 2015; Nishi et al. 2017; Thompson et al. 2017; Nishi et al. 2020; Tsuchiya et al. 2008; Tsuchiya and Tsuchiya 2011)

(2018). The phase transition from pyrite-type to $P\bar{4}2_1m$ (YbOOH-type structure) has been suggested to occur in InOOH at ∼50 GPa. Interestingly, $P\bar{4}2_1m$-InOOH has asymmetric hydrogen bonds in the structure and the coordination number of In is 7 from 50 to 90 GPa (Figs. 4 and 5, Table 2). $P\bar{4}2_1m$-InOOH dissociates into In_2O_3 + H_2O (ice) above about 80 GPa. In the case of AlOOH composition, however, the free energy of this type of structure is higher than the dissociation products Al_2O_3 +H_2O throughout the pressure range investigated (100–500 GPa).

2.6 Hydrogen bond symmetrization

Usually, in hydrous oxide minerals, a hydrogen bond is formed by a hydrogen atom covalently bonded to a highly electronegative atom such as oxygen (O–H), with the non-covalent electron pair of another oxygen to form O· · ·H. Hydrogen bonds are usually much weaker than covalent or ionic bonds. However, their strength varies depending on the surrounding chemical and physical environments. In general, the stronger the hydrogen bond (O· · ·H) is, the longer the O–H distance is (Fig.3). Also, the closer the O–H· · ·O angle is to 180°, the stronger the hydrogen bond is (Brown 1976). As the hydrogen bonds become stronger under high pressure, the O· · ·O distance decreases, while the O–H bond distance increases (Figs. 3 and 4). Eventually, with increased

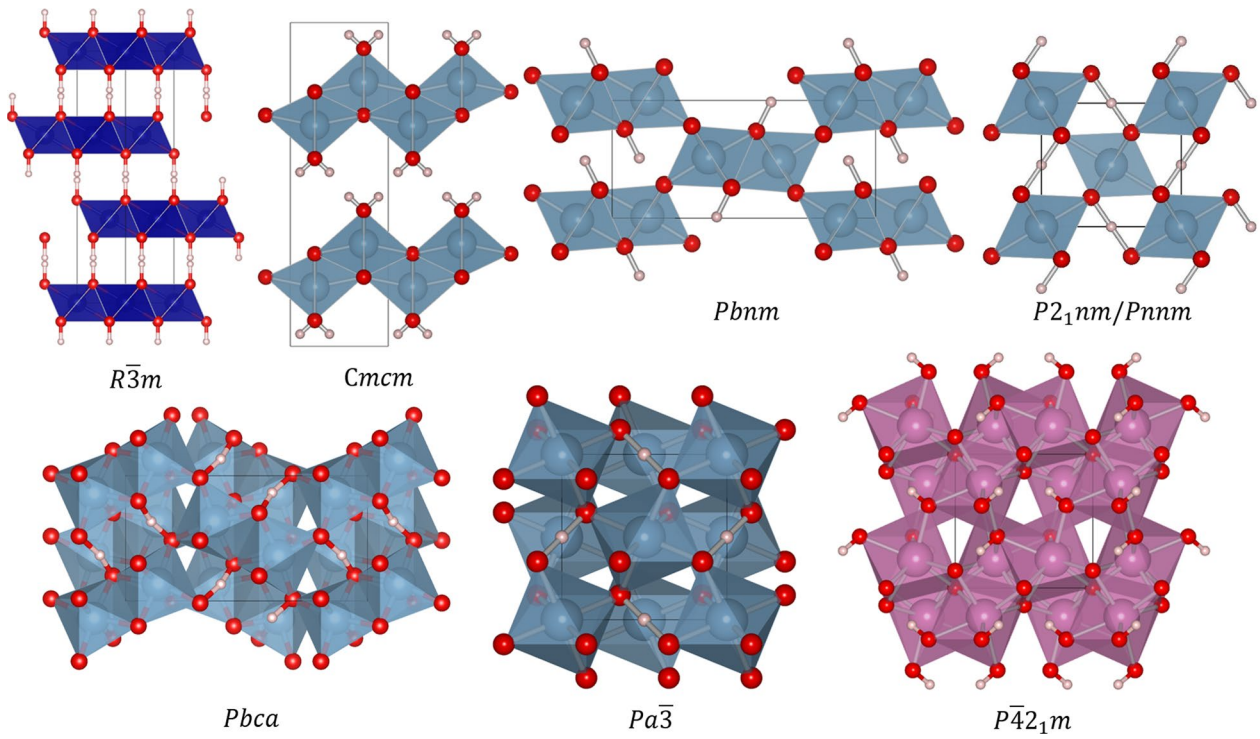

Fig. 5 Variety of the crystal structures of Oxyhydroxide MOOH

pressure the hydrogen atom moves to the midpoint between two neighboring oxygen atoms and is strongly bonded to both of these oxygen atoms. This entire process is called pressure-induced hydrogen bond symmetrization, and the resulting bond is referred to as a symmetric hydrogen bond.

Many theoretical studies have been conducted to understand the behavior of protons in water ice at high pressure, resulting in the identification of pressure-induced hydrogen bond symmetrization in high-pressure ice polymorphs (Holzapfel 1972; Schweizer and Stillinger 1984). The hydrogen bond symmetrization of ice phases can be divided into five main stages (Fig. 3). Under low pressure and low temperature conditions, the potential surface between oxygen atoms (O···O) is asymmetric, and the proton is covalently bonded to the oxygen atom and weakly hydrogen bonded to the other oxygen atom (e.g., ice VIII, Fig. 3, part 1). On the other hand, above approximately 270 K, ice VIII transform to ice VII, which is stable with statically disordered protons due to an order-disorder transition (Fig. 3, part 2). In both ice VII and ice VIII, the potential barrier between the oxygen atoms is lowered under high pressure (>40 GPa), and the protons change to a dynamically disordered state due to thermal vibrations and quantum tunneling effects (Benoit et al. 1998, 2002). In this state, when the proton distribution is bimodal/unimodal, the ice phase is called dynamically disordered ice VII/X (Fig. 3, part 3 and 4). Finally, at pressures exceeding ~100–120 GPa, the potential surface changes to a single minimum by compression, and the protons are located at the middle point of the two oxygen atoms (ice X, Fig. 3, part 5). This final stage represents a completely symmetrized hydrogen bond.

Pressure-induced hydrogen bond symmetrization has been both predicted and experimentally observed in potential deep Earth phases as well. The pressure dependence of hydrogen positions in δ-AlOOH was investigated using ab initio calculations, and these results suggested the possibility of hydrogen bond symmetrization at pressures of about 30 GPa at static 0 K condition (Tsuchiya et al. 2002). This symmetrization is coincident with a second-order phase transition from the $P2_1nm$ to $Pnnm$ symmetry and a significant increase in the bulk modulus. Subsequent neutron diffraction experiments found that at ambient temperature, the $P2_1nm$ to $Pnnm$ phase transition of δ-AlOOH occurs at ~9 GPa and the symmetrization of hydrogen bond was observed above 18.1 GPa (Sano-Furukawa et al. 2018). Recently, ab initio calculations and nuclear magnetic resonance (NMR) experiments on δ-AlOOH were carried out at pressures up to 40 GPa. They concluded that the structural transition from $P2_1nm$ to $Pnnm$ occurs at ~10 GPa and that hydrogen bond symmetrization occurs at 14.7 GPa without going through a proton tunneling state in that process because the calculated potential surface was single minimum and no energy barrier existed (Trybel et al. 2021).

Like δ-AlOOH, ab initio calculations show that Mg-endmember phase D ($MgSi_2O_6H_2$) undergoes hydrogen bond symmetrization at pressures above 40–45 GPa (Tsuchiya et al. 2005a; Thompson et al. 2022). Al-endmember phase D is also calculated to undergo hydrogen bond symmetrization at pressures of approximately 40 GPa (Thompson et al. 2022), although interestingly, in non-endmember compositions of Al-bearing phase D not all bonds appear to undergo pressure-dependent hydrogen bond symmetrization (Panero and Caracas 2020; Thompson et al. 2022). Hydrogen bond symmetrization has been shown to have a marked effect on the optical and elastic properties of both the Mg- and Al-endmember compositions of phase D (Tsuchiya et al. 2008; Tsuchiya and Tsuchiya 2008, 2009; Thompson et al. 2022). More broadly, pressure-induced hydrogen bond symmetrization has been computationally predicted and/or experimentally observed in many potential hosts of hydrogen in Earth's lower mantle, including δ-AlOOH, phase D, and ϵ-FeOOH (see below). Pyrite-type FeOOH and AlOOH do not undergo pressure-induced hydrogen bond symmetrization as their hydrogen bonds are already symmetric at the onset of their stability. Based on the dominance of symmetric hydrogen bonding in hydrous mantle phases, the formation of very strong hydrogen bonds is assumed to contribute to the stabilization of the crystal structure of hydrous minerals under the high-pressure conditions of the lower mantle.

2.7 Symmetric hydrogen bonds in the deep Earth

Of the hydrous lower mantle phases, phase D, phase H, and all of $CaCl_2$-type and pyrite-type MOOH (M=Al, Fe, In), phases discussed herein contain symmetric hydrogen bonds. In the case of some of these phases (e.g., δ-AlOOH, ϵ-FeOOH, phase D, and phase H), symmetric hydrogen bonds were achieved through the process of pressure-induced hydrogen bond symmetrization. In contrast, pyrite-type MOOH (M=Al, Fe, In) phases contain symmetric bonds at the onset of their formation by virtue of their innate symmetry. Fig. 4 shows how the distance between the covalently bonded oxygen and hydrogen atoms (R_{OH}) and the hydrogen bond angle (O–H···O) vary with the oxygen–oxygen distance ($R_{O\cdots O}$) in InOOH, AlOOH, FeOOH, and DHMSs under pressure. In this figure, symmetric bonds can be identified when $R_{O\cdots H} \sim 2.4$ Å and O–H···O angle is 180°. Furthermore, a recent study using in situ ^{1}H-NMR to probe ice, Fe- and Al-bearing phase D, and δ-(Al,Fe)OOH at high pressure has reported that the NMR resonance line-width has

a minima around R_{OO} ~2.44–2.45 Å, regardless of the chemical composition (Meier et al. 2022). This minimum is interpreted to be associated with a hydrogen mobility maximum which is explained as a precursor to a localization of hydrogen atoms (i.e., the symmetrization of the potential surface between oxygen atoms).

It is worth noting that while the aforementioned deep Earth phases exhibit symmetric hydrogen bonding at lower mantle pressures, some hydrous minerals do not undergo hydrogen bond symmetrization even when pressurized to ultra-high-pressure conditions. For example, this behavior is shown by *Pbnm*-AlOOH (diaspore) even when pressurized up to ~100 GPa, which is well beyond the conditions at which it is thermodynamically stable (Fig. 4). This is due to the shape of potential surface between oxygen atoms resulting from the symmetry of the crystal structure. Another example is *Pbca*-AlOOH, which is stable only in a relatively narrow pressure region (Fig. 4). The inability to produce symmetric hydrogen bonds is interpreted to be due to the fact that the hydrogen bonding angle tends to be smaller (170° to 165°), which renders the hydrogen bonding weaker under pressure.

2.8 Vibrational properties of hydrogen bond symmetrization and dynamically disordering state

Many studies have probed the changes in optical and vibrational properties associated with hydrogen bond symmetrization in ice phases (e.g., Goncharov et al. 1996, 1999; Aoki et al. 1996; Song et al. 2003). Most of these studies report that the OH-stretching vibration observed around 3500 cm^{-1} at ambient pressure decreases rapidly with increasing pressure and then gradually increases again at about 60 GPa. Based on the sudden change of the vibrational properties at ~60 GPa, the transition from ice VII/VIII to ice X was estimated to occur at ~60 GPa. On the other hand, Caracas (2008) showed that the phonon in the ice X phase softens below about 120 GPa, indicating that the structure of ice X is unstable. That soft mode in ice X corresponds to the double-well potential between oxygen atoms, where protons can move back and forth on that double-well potential. That unstable phonon mode suggests the transition from ice X to dynamically disordered ice VII by decompression below 120 GPa, even at 0 K. Sugimura et al. (2008) reported the ice VII undergoes a change in compressibility at 40 and 60 GPa at room temperature, corresponding to the phase transitions from ice VII to dynamically disordered ice VII (~40 GPa) and subsequently to the dynamically disordered ice X phase (~60 GPa) (Fig. 3). The equation of state of ice VII phase was investigated by first principles centroid molecular dynamics simulation incorporating thermal vibration and NQE (Ikeda 2018). The NQE causes a slight increase in the compressibility of ice VII near about 30–60 GPa, but this is not enough to explain the experimental observation. The effects of NQE in ice VII were also investigated by high-pressure H^1-NMR study (Meier et al. 2018). They reported the proton tunneling mode was observed from 20 to 75 GPa.

The ab initio static 0 K calculation results show that the OH-stretching frequencies of δ-AlOOH with the proton-ordered model decrease significantly from ~2700 to ~1700 cm^{-1} with increased pressure up to 30 GPa, at which point hydrogen bond symmetrization occurs and then the corresponding vibrational modes increase gradually under higher pressure (Tsuchiya et al. 2008). Raman spectroscopy measurements of the OH vibrations in δ-AlOOH at ambient conditions (Ohtani et al. 2001a) have reported four broad bands between 2000 and 2800 cm^{-1}, indicating the strong and asymmetric hydrogen bonds with multiple hydrogen positions. Ab initio calculations show that these Raman scattering bands can be explained by the partial disordering of proton in δ-AlOOH at 300 K (Tsuchiya et al. 2008). The pressure dependence of the lattice mode (350–700 cm^{-1}) was measured up to 89.5 GPa at room temperature using Brillouin spectroscopy combined with high-pressure Raman spectroscopic measurements in a diamond anvil cell on δ-AlOOH (Mashino et al. 2016). The pressure dependence of the Raman frequencies indicates the transition from $P2_1nm$ to *Pnnm* occurs at 5.6 GPa. Recently, ab initio calculation results have been reported that explain the several experimental features caused by the change of the proton dynamics under pressure (Luo et al. 2022). As we approach the pressure of hydrogen bond symmetrization, anharmonicity and quantum tunneling effects become more important in proton dynamics. Therefore, in order to elucidate proton dynamics in pressure-induced hydrogen bond symmetrization, these effects need to be investigated in more detail.

2.9 Effects of hydrogen bond symmetrization on the elasticity of hydrous minerals

The effect of pressure-induced hydrogen bond symmetrization on the elastic properties of hydrous minerals and high-pressure ice phases has been studied using ab initio calculations (Tsuchiya et al. 2008; Tsuchiya and Tsuchiya 2009, 2017; Thompson et al. 2017, 2021, 2022). According to these calculations performed under static 0 K conditions, the elastic constants are reported to increase rapidly with hydrogen bond symmetrization. Recently, elastic properties of hydrous minerals and ice phases have also been studied by Brillouin scattering experiments at high pressures (e.g., Mashino et al. 2016; Ohira et al. 2021; Satta et al. 2021; Zhang et al. 2019). These results are in general agreement with theoretical

calculations, but the rapidness of the increase in the elastic constants at the onset of hydrogen bond symmetrization seems to be suppressed.

Figure 6 shows a comparison of the pressure dependence of the elastic constants of high-pressure ice polymorphs determined using theoretical calculations at static 0 K and experimental measurements conducted at ambient temperature (Tsuchiya and Tsuchiya 2017; Zhang et al. 2019; Shi et al. 2021; Ahart et al. 2011). There is good agreement between theoretical calculations of asymmetric hydrogen bonding and experimental results of single-crystal Brillouin scattering up to pressures up to about 50 GPa. On the other hand, the experimental results are somewhat higher for higher pressure conditions. In this pressure region, a dynamically disordered state of protons has been reported in ice VII (Sugimura et al. 2008; Caracas 2008). In this dynamically disordered state, protons move back and forth over the double minimum potential between two oxygen atoms due to thermal and quantum vibration. The evolution of the elastic properties as a function of pressure indicates that the elastic constants approach the symmetric hydrogen bonding state due to the instantaneous hydrogen bonding symmetrization of some protons. From this point of view, this state can be regarded as a dynamic symmetrization of the hydrogen bond. Although experimental results above 100 GPa, where the potential surface changes to a single minimum, have not yet been reported, we expect to see a decrease in the pressure gradient of the experimental elastic constants, perhaps following a pressure dependence similar to that observed in the calculations.

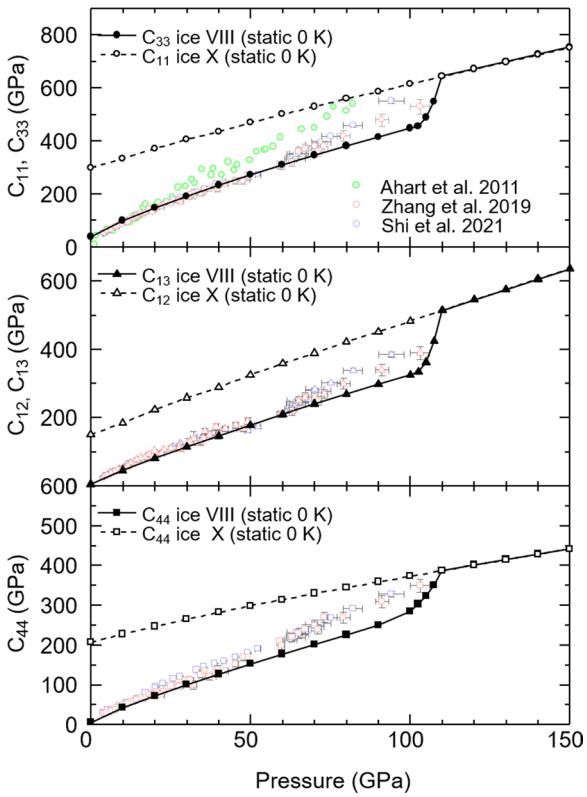

Fig. 6 The calculated and experimental elastic constants of high-pressure ice VIII, VII, and X (Tsuchiya and Tsuchiya 2017; Zhang et al. 2019; Shi et al. 2021; Ahart et al. 2011). The full lines with full symbols indicate the calculated elastic constants of ice VIII containing asymmetric hydrogen bond. Dashed lines indicate the elastic constants of ice X with symmetric hydrogen bond. Note that ice VIII and ice VII have tetragonal and cubic crystal symmetries, respectively, and the index of the elastic constants are different (e.g., C_{33} of ice VIII corresponds to C_{11} in ice VII and X)

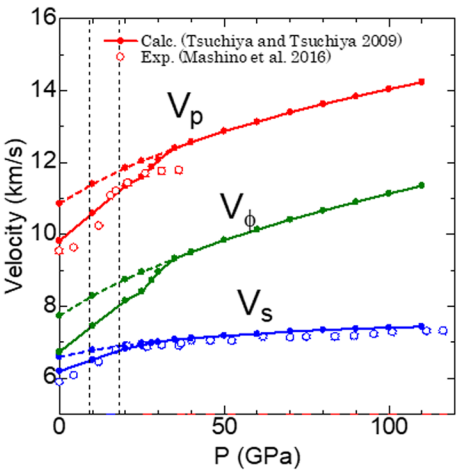

Fig. 7 The calculated and experimental velocities (Tsuchiya and Tsuchiya 2009; Mashino et al. 2016) of δ-AlOOH. Dashed lines indicate the pressure conditions where symmetry change (9 GPa) and hydrogen bond symmetrization (18 GPa) were observed experimentally (Sano-Furukawa et al. 2008, 2018)

High-pressure acoustic wave velocity measurements of δ-AlOOH using Brillouin spectroscopy also show good agreement with theoretical elasticity calculations (Mashino et al. 2016) (Fig. 7). Pressure-induced hydrogen bond symmetrization is reported to occur at ambient temperature and ~18 GPa (Sano-Furukawa et al. 2018). The second-order phase transition of δ-AlOOH from the $P2_1nm$ to $Pnnm$ symmetry is reported to occur at ~9 GPa (Sano-Furukawa et al. 2008). This symmetry change is presumably caused by the change from the ordered to disordered state of the proton in δ-AlOOH. Therefore, the change from static to dynamic disordering state of protons is expected to occur between 9 GPa and 18 GPa. Due to the scattered data points at these pressure condition, it is unclear if there is a change of the acoustic wave velocities under pressure caused by the dynamically disordered state.

3 Conclusions

This paper reviews theoretical and experimental studies of the stability, structure, and physical properties of hydrous minerals with symmetric hydrogen bonding which may be found in the Earth's lower mantle and provides an overview of pressure-induced hydrogen bond symmetrization. In mantle phases that undergo pressure-induced hydrogen bond symmetrization, the behavior of protons is qualitatively similar to that of well-studied high-pressure ice phases. However, the pressure at which pressure-induced hydrogen bond symmetrization occurs is lower in these mantle phases than in ice polymorphs, and therefore it is more experimentally accessible to study proton dynamics in these phases. However, hydrous minerals are more compositionally complex than H_2O ices, which can present experimental challenges such as multiple, difficult to deconvolve vibrational OH modes. Furthermore, the hydrous phases discussed here may form different solid solutions depending on the composition, pressure, and temperature (*X-P-T*) of that system. For example, $CaCl_2$-structured compositions intermediate to the phase H, AlOOH, and FeOOH-endmembers could coexist with pyrite-type (Al,Fe)OOH due to the strong influence of cation substitution on the thermodynamic stability of these phases. Additional research is needed to probe the stability, hydrogen bonding, and geophysical properties of these intermediate compositions which are likely to coexist in the lower mantle. Since the temperature effect and the tunneling effect both drive the appearance of dynamically disordered states, the pressure conditions at which the dynamically disordered state appears may decrease at higher temperatures. Changes in the vibrational and the elastic properties accompanying the transition to the dynamically disordered state should be examined in the future. Lastly, we hope this review leads to a better understanding of hydrogen dynamics and the role of theoretical ab initio studies in predicting and constraining the stability and properties of high-pressure hydrous minerals moving forward.

Abbreviations

DHMSs: Dense hydrous magnesium silicates; NAMs: Nominally anhydrous minerals; CMB: Core–mantle boundary; NQE: Nuclear quantum effect; NMR: Nuclear magnetic resonance.

Author contributions

JT proposed the topic. JT and ET contributed equally to writing the review. Both authors read and approved the final manuscript.

Funding

This work was supported by JSPS KAKENHI Grant Number JP20K04043 and JP20K04126.

Availability of data and materials

Not applicable.

Declarations

Competing interest

The authors declare that they have no competing interest.

Author details

[1]Geodynamics Research Center, Ehime University, 2-5 Bunkyo-cho, Matsuyama, Ehime 790-8577, Japan. [2]Department of Earth and Environmental Systems, The University of the South, 735 University Avenue, Sewanee, TN 37383, USA.

Received: 1 September 2022 Accepted: 19 October 2022
Published online: 17 November 2022

References

Ahart M, Somayazulu M, Gramsch SA, Boehler R, Mao H-K, Hemley RJ (2011) Brillouin scattering of h_2o ice to megabar pressures. J Chem Phys 134:124517. https://doi.org/10.1063/1.3557795

Albarede F (2009) Volatile accretion history of the terrestrial planets and dynamic implications. Nature 461:1227–1233. https://doi.org/10.1038/nature08477

Aoki K, Yamawaki H, Sakashita M, Fujihisa H (1996) Infrared absorption study of the hydrogen-bond symmetrization in ice to 110 GPa. Phys Rev B 54:15673–15677

Baroni S, de Gironcoli S, Dal Corso A (2001) Phonons and related crystal properties from density-functional perturbation theory. Rev Mod Phys 73:515–562

Benoit M, Marx D, Parrinello M (1998) Tunnelling and zero-point motion in high-pressure ice. Nature 392:258–261

Benoit M, Romero AH, Marx D (2002) Reassigning hydrogen-bond centering in dense ice. Phys Rev Lett 89:145501. https://doi.org/10.1103/PhysRevLett.89.145501

Bercovici D, Karato S-I (2003) Whole-mantle convection and the transition-zone water filter. Nature 425:39–44

Brown ID (1976) On the geometry of o–h ⋯ o hydrogen bonds. Acta Crystallogr Sect A 32(1):24–31. https://doi.org/10.1107/S0567739476000041

Buchen J, Sturhahn W, Ishii T, Jackson JM (2021) Vibrational anisotropy of *δ*-(Al,Fe)OOH single crystals as probed by nuclear resonant inelastic X-ray scattering. Eur J Mineral 33:485–502

Busing WR, Levy HA (1958) A single crystal neutron diffraction study of diaspore AlO(OH). Acta Cryst 11:798–803

Caracas R (2008) Dynamical instabilities of ice x. Phys Rev Lett 101:085502. https://doi.org/10.1103/PhysRevLett.101.085502

Christensen AN, Hazell RG (1972) The crystal structure of the tetragonal modification of YbOOH. Acta Chem Scand 26:1171–1176

Christensen AN, Hansen P, Lehmann MS (1976) Isotopic effects in the bonds of *β*-CrOOH and *β*-CrOOD. J Solid State Chem 19:299–304

Christensen AN, Hansen P, Lehmann MS (1977) Isotopic effects in the bonds of *α*-CrOOH and *α*-CrOOD. Acta Chem Scand 21:325–329

Cococcioni M, de Gironcoli S (2005) Linear response approach to the calculation of the effective interaction parameters in the LDA+U method. Phys Rev B 71:035105

Corbato CE, Tettenhorst T, Ghristoph GG (1985) Structure refinement of deuterated boehmite. Clay Clay Miner 1:71–75

Giannozzi P, Baroni S, Bonini N, Calandra M, Car R, Cavazzoni C, Ceresoli D, Chiarotti GL, Cococcioni M, Dabo I, Dal Corso A, de Gironcoli S, Fabris S, Fratesi G, Gebauer R, Gerstmann U, Gougoussis C, Kokalj A, Lazzeri M, Martin-Samos L, Marzari N, Mauri F, Mazzarello R, Paolini S, Pasquarello A, Paulatto L, Sbraccia C, Scandolo S, Sclauzero G, Seitsonen AP, Smogunov A, Umari P, Wentzcovitch RM (2009) Quantum espresso: a modular and open-source software project for quantum simulations of materials. J Phys: Condens Matter 21:395502. https://doi.org/10.1088/0953-8984/21/39/395502

Glasser LSD, Ingram L (1968) Refinement of the crystal structure of groutite, *α*-MnOOH. Acta Cryst B24:1233–1236

Gleason AE, Quiroga A, Suzuki A, Pentcheva R, Mao WL (2013) Symmetrization driven spin transition in ϵ-FeOOH at high pressure. Earth Planet Sci Lett 379:49–44

Goncharov AF, Struzhkin VV, Somayazulu MS, Hemley RJ, Mao HK (1996) Compression of ice to 210 Gigapascals: infrared evidence for a symmetric hydrogen-bonded phase. Science 273:218–220. https://doi.org/10.1126/science.273.5272.218

Goncharov AF, Struzhkin VV, Mao HK, Hemley RJ (1999) Raman spectroscopy of dense H_2O and the transition to symmetric hydrogen bonds. Phys Rev Lett 83:1998–2001

Hirschmann MM (2006) Water, melting, and the deep Earth H_2O cycle. Annu Rev Earth Planet Sci 34:629–653. https://doi.org/10.1146/annurev.earth.34.031405.125211

Hirschmann M, Kohlstedt D (2012) Water in Earth's mantle. Phys Today 65(3):40. https://doi.org/10.1063/PT.3.1476

Holzapfel WB (1972) On the symmetry of the hydrogen bonds in ice VII. J Chem Phys 56:712–715

Hu Q, Kim D, Liu J, Meng Y, Yang L, Zhang D, Mao WL, Mao H-K (2017) Dehydrogenation of goethite in Earth's deep lower mantle. Proc Natl Acad Sci USA 114:1498–1501

Ikeda T (2018) First principles centroid molecular dynamics simulation of high pressure ices. J Chem Phys 148:102332. https://doi.org/10.1063/1.5003055

Inoue T (2000) Water in the Earth's interior-is the mantle transition zone a water reservoir? Rev High Press Sci Technol 10:124–133

Kawazoe T, Ohira I, Ishii T, Boffa Ballaran T, McCammon C, Suzuki A, Ohtani E (2017) Single crystal synthesis of δ-(Al, Fe)OOH. Am Miner 102:1953–1956

Kohler T, Armbruster T, Libowitzxky E (1997) Hydrogen bonding and Jahn–Teller distortion in groutite, α-MnOOH], and manganite, γ-MnOOH, and their relations to the manganese dioxides ramsdellite and pyrolusite. J Solid State Chem 133:486–500

Kuwayama Y, Hirose K, Sata N, Ohishi Y (2005) The pyrite-type high-pressure form of silica. Science 309:923–925. https://doi.org/10.1126/science.1114879

Lehmann MS, Larsen FK, Poulsen FR, Christensen AN, Rasmussen SE (1970) X-ray crystallographic studies on indium oxide hydroxide. Acta Chem Scand 24:1662–1670

Liu L (1986) Phase transformation in serpentine at high pressures and temperatures and implications for subducting lithosphere. Phys Earth Planet Inter 42:255–262

Luo C, Umemoto K, Wentzcovitch RM (2022) Ab initio investigation of h-bond disordering in δ-AlOOH. Phys Rev Res 4:023223. https://doi.org/10.1103/PhysRevResearch.4.023223

Mashino I, Murakami M, Ohtani E (2016) Sound velocities of δ-AlOOH up to core-mantle boundary pressures with implications for the seismic anomalies in the deep mantle. J Geophys Res: Solid Earth 121:595–609. https://doi.org/10.1002/2015JB012477

Meier T, Petitgirard S, Khandarkhaeva S, Dubrovinsky L (2018) Observation of nuclear quantum effects and hydrogen bond symmetrisation in high pressure ice. Nature Comm 9:2766. https://doi.org/10.1038/s41467-018-05164-x

Meier T, Trybel F, Khandarkhaeva S, Laniel D, Ishii T, Aslandukova A, Dubrovinskaia N, Dubrovinsky L (2022) Structural independence of hydrogen-bond symmetrisation dynamics at extreme pressure conditions. Nature Comm 13:3042. https://doi.org/10.1038/s41467-022-30662-4

Milton C, Appleman DE, Appleman MH, Chao ECT, Cuttitta F, Dinnin JI, Dwornik EJ, Ingram BL, Rose HJJ (1976) Merumite, a complex assemblage of chromium minerals from Guyana. U.S. Geological Survey Professional Paper 887:1–29

Mookherjee M, Tsuchiya J (2015) Elasticity of superhydrous phase, B, $Mg_{10}Si_3O_{14}(OH)_4$. Phys Earth Planet Inter 238:42–50. https://doi.org/10.1016/j.pepi.2014.10.010

Nishi M, Irifune T, Tsuchiya J, Tange Y, Nishihara Y, Fujino K, Higo Y (2014) Stability of hydrous silicate at high pressures and water transport to the deep lower mantle. Nat Geophys 7:224–227. https://doi.org/10.1038/ngeo2074

Nishi M, Kuwayama Y, Tsuchiya J (2017) The pyrite-type high-pressure form of FeOOH. Nature 547:205–208. https://doi.org/10.1038/ngeo22823

Nishi M, Tsuchiya J, Arimoto T, Kakizawa S, Kunimoto T, Tange Y, Higo Y, Irifune T (2018) Thermal equation of state of $MgSiO_4H_2$ phase H determined by in situ X-ray diffraction and a multianvil apparatus. Phys Chem Miner 45:995–1001. https://doi.org/10.1007/s00269-018-09870-z

Nishi M, Kuwayama Y, Tsuchiya J (2020) New aluminum hydroxide at multi-megabar pressures: implications for water reservoirs in deep planetary interiors. Icarus 338:113539. https://doi.org/10.1016/j.icarus.2019.113539

Ohira I, Ohtani E, Sakai T, Miyahara M, Hirao N, Ohishi Y, Nishijima M (2014) Stability of a hydrous δ-phase, AlOOH-$MgSiO_2(OH)_2$, and a mechanism for water transport into the base of lower mantle. Earth Planet Sci Lett 401:12–17

Ohira I, Jackson JM, Solomatova NV, Sturhahn W, Finkelstein GJ, Kamada S, Kawazoe T, Maeda F, Hirawo N, Nakano S, Toeller TS, Suzuki A, Ohtani E (2019) Compressional behavior and spin state of δ-(Al, Fe)OOH at high pressures. Am Miner 104:1273–1284. https://doi.org/10.2138/am-2019-6913

Ohira I, Jackson JM, Sturhahn W, Finkelstein G, Kawazoe T, Toellner TS, Suzuki A, Ohtani E (2021) The influence of δ-(Al, Fe)OOH on seismic heterogeneities in earth's lower mantle. Sci Rep 11:12036. https://doi.org/10.1038/s41598-021-91180-9

Ohtani E (2020) The role of water in Earth's mantle. Natl Sci Rev 7:224–232

Ohtani E, Litasov K, Suzuki A, Kondo T (2001) Stability field of new hydrous phase, δ-AlOOH, with implications for water transport into the deep mantle. Geophys Res Lett 28:3991–3993

Ohtani E, Toma M, Litasov K, Kubo T, Suzuki A (2001) Stability of dense hydrous magnesium silicate phases and water storage capacity in the transition zone and lower mantle. Earth Planet Sci Lett 124:105–117

Ohtani E, Amaike Y, Kamada S, Sakamaki T, Hirao N (2014) Stability of hydrous phase H $MgSiO_4H_2$ under lower mantle conditions. Geophys Res Lett 41:8283–8287. https://doi.org/10.1002/2014GL061690

Ono S (1998) Stability limits of hydrous minerals in sediment and mid-ocean ridge basalt compositions: implications for water transport in subduction zones. J Geophys Res 103:18253–18267

Ono S, Tsuchiya T, Hirose K, Ohishi Y (2003) High-pressure form of pyrite-type germanium dioxide. Phys Rev B 68:014103. https://doi.org/10.1103/PhysRevB.68.014103

Oosterhout WV (1960) Morphology of synthetic submicroscopic crystals and α and γ-FeOOH and γ-Fe_3O_3 prepared from FeOOH. Acta Cryst 13:932–935

Pamato MG, Myhill R, Boffa Ballaran T, Frost DJ, Heidelbach F, Miyajima N (2014) Lower-mantle water reservoir implied by the extreme stability of a hydrous aluminosilicate. Nat Geosci 8:75–79. https://doi.org/10.1038/NGEO2306

Panero WR, Caracas R (2017) Stability of phase H in the $MgSiO_4H_2$-AlOOH-SiO_2 system. Earth Planet Sci Lett 463:171–177. https://doi.org/10.1016/j.epsl.2017.01.033

Panero WR, Caracas R (2020) Stability and solid solutions of hydrous aluminosilicates in the Earth's mantle. Minerals 10:330. https://doi.org/10.3390/min10040330

Pearson DG, Brenker FE, Nestola F, McNeill J, Nasdala L, Hutchison MT, Matveev S, Mather K, Silversmit G, Schmitz S, Vekemans B, Vincze L (2014) Hydrous mantle transition zone indicated by ringwoodite included within diamond. Nature 507:221–226. https://doi.org/10.1038/nature13080

Pernet M, Joubert JC, Berthet-Colominas C (1975) Etude per diffraction neutronique de la forme haute pression de FeOOH. Solid State Commun 17:1505–1510

Ringwood AE, Major A (1967) High-pressure reconnaissance investigations in the system Mg_2SiO_4-MgO-H_2O. Earth Planet Sci Lett 2:130–133

Sampson CF (1969) The lattice parameter of natural single crystal and synthetically produced goethite (α-FeOOH). Acta Cryst B25:1683–1685

Sano-Furukawa A, Komatsu K, Vanpeteghem CB, Ohtani E (2008) Neutron diffraction study of δ-AlOOH at high pressure and its implication for symmetrization of the hydrogen bond. Am Miner 93(10):1558–1567. https://doi.org/10.2138/am.2008.2849

Sano-Furukawa A, Hattori T, Komatsu K, Kagi H, Nagai T, Molaison JJ, dos Santos AM, Tulk CA (2018) Direct observation of symmetrization of hydrogen bond in δ-AlOOH under mantle conditions using neutron diffraction. Sci Rep 8:15520. https://doi.org/10.1038/s41598-018-33598-2

Sano A, Ohtani E, Kondo T, Hirao N, Sakai T, Sata N, Ohishi Y, Kikegawa T (2008) Aluminous hydrous mineral δ-AlOOH as a carrier of hydrogen into the core-mantle boundary. Geophys Res Lett 35:03303. https://doi.org/10.1029/2007GL031718

Sano A, Yagi T, Okada T, Gotou H, Ohtani E, Tsuchiya J, Kikegawa T (2008) X-ray diffraction study of high pressure transition in InOOH. J Miner Petrol Sci 103:152–155. https://doi.org/10.2465/jmps.071002m

Satta N, Criniti G, Kurnosov A, Boffa Ballaran T, Ishii T, Marquardt H (2021) High-pressure elasticity of δ-(Al, Fe)OOH single crystals and seismic detectability of hydrous MORB in the shallow lower mantle. Geophys Res Lett 48:2021–094185. https://doi.org/10.1029/2021GL094185
Schmidt MW, Poli S (1998) Experimentally based water budgets for dehydrating slabs and consequences for arc magma generation. Earth Planet Sci Lett 163:361–379
Schweizer KS, Stillinger FH (1984) High pressure phase transitions and hydrogen-bond symmetry in ice polymorphs. J Chem Phys 80:1230–1240
Shieh S, Mao H-K, Hemley RJ, Ming LC (2000) In situ X-ray diffraction studies of dense hydrous magnesium silicates at mantle conditions. Earth Planet Sci Lett 177:69–80
Shi W, Sun N, Li X, Mao Z, Liu J, Prakapenka VB (2021) Single-crystal elasticity of high-pressure ice up to 98 GPa by brillouin scattering. Geophys Res Lett 48:2021–092514. https://doi.org/10.1029/2021GL092514
Smyth JR (1994) A crystallographic model for hydrous wadsleyite (β-Mg_2SiO_4): an ocean in the earth's interior? Am Miner 79:1021–1024
Song M, Yamawaki H, Fujihisa H, Sakashita M, Aoki K (2003) Infrared investigation on ice VIII and the phase diagram of dense ices. Phys Rev B 68:014106. https://doi.org/10.1103/PhysRevB.68.014106
Sugimura E, Iitaka T, Hirose K, Kawamura K, Sata N, Ohishi Y (2008) Compression of H_2O ice to 126 GPa and implications for hydrogen-bond symmetrization: synchrotron x-ray diffraction measurements and density-functional calculations. Phys Rev B 77:214103. https://doi.org/10.1103/PhysRevB.77.214103
Suzuki A, Ohtani E, Kamada T (2000) A new hydrous phase δ-AlOOH synthesized at 21 GPa and 1000 °C. Phys Chem Miner 27:689–693
Suzuki A, Ohtani E, Kamada T (2021) Spectroscopic evidence for the fe3+ spin transition in iron-bearing δ-AlOOH at high pressure. Am Miner 106:1709–1716
Thompson EC, Campbell AJ, Tsuchiya J (2017) Elasticity of ϵ-FeOOH: seismic implications for Earth's lower mantle. J Geophys Res: Solid Earth 122:5038–5047. https://doi.org/10.1002/2007JB014168
Thompson EC, Davis AH, Brauser NM, Liu Z, Prakapenka VB, Campbell AJ (2020) Phase transitions in ϵ-FeOOH at high pressure and ambient temperature. Am Miner 105:1769–1777. https://doi.org/10.2138/am-2020-7468
Thompson EC, Campbell AJ, Tsuchiya J (2021) Elastic properties of the pyrite-type FeOOH–AlOOH system from first principles calculations. Geochem Geophys Geosyst 22:2021–009703. https://doi.org/10.1029/2021GC009703
Thompson EC, Campbell AJ, Tsuchiya J (2022) Calculated elasticity of Al-bearing phase D. Minerals 12:922. https://doi.org/10.3390/min12080922
Trybel F, Meier T, Wang B, Steinle-Neumann G (2021) Absence of proton tunneling during the hydrogen-bond symmetrization in δ-AlOOH. Phys Rev B 104:104311. https://doi.org/10.1103/PhysRevB.104.104311
Tsuchiya J (2013) First principles prediction of a new high-pressure phase of dense hydrous magnesium silicates in the lower mantle. Geophys Res Lett 40:4570–4573. https://doi.org/10.1002/grl.50875
Tsuchiya J, Tsuchiya T (2017) First principles calculation of the elasticity of ice VIII and X. J Chem Phys 146:024501. https://doi.org/10.1063/1.4973339
Tsuchiya J, Tsuchiya T (2008) Elastic properties of phase D ($MgSi_2O_6H_2$) under pressure: Ab initio investigation. Phys Earth Planet Inter 170:215–220. https://doi.org/10.1016/j.pepi.2008.05.015
Tsuchiya J, Tsuchiya T (2009) Elastic properties of δ-AlOOH under pressure: first principles investigation. Phys Earth Planet Inter 174:122–127. https://doi.org/10.1016/j.pepi.2009.01.008
Tsuchiya J, Umemoto K (2019) First-principles determination of the dissociation phase boundary of phase H $MgSiO_4H_2$. Geophys Res Lett 46:7333–7336. https://doi.org/10.1029/2019GL083472
Tsuchiya J, Tsuchiya T, Tsuneyuki S, Yamanaka T (2002) First principles calculation of a high-pressure hydrous phase, δ-AlOOH. Geophys Res Lett 29:1909. https://doi.org/10.1029/2002GL015417
Tsuchiya J, Tsuchiya T, Tsuneyuki S (2005) First principles study of hydrogen bond symmetrization of phase D under high pressure. Am Miner 90:44–49. https://doi.org/10.2138/am.2005.1628
Tsuchiya J, Tsuchiya T, Wentzcovitch RM (2005) Transition from the Rh_2O_3(II)-to-$CaIrO_3$ structure and the high-pressure-temperature phase diagram of alumina. Phys Rev B 72:020103. https://doi.org/10.1103/PhysRevB.72.020103
Tsuchiya J, Tsuchiya T, Wentzcovitch RM (2008) Vibrational properties of δ-AlOOH under pressure. Am Miner 93:447–482. https://doi.org/10.2138/am.2008.2627
Tsuchiya J, Tsuchiya T, Sano A, Ohtani E (2008) First principles prediction of new high-pressure phase of InOOH. J Miner Petrol Sci 103:116–120. https://doi.org/10.2465/jmps.071022e
Tsuchiya J, Tsuchiya T (2011) First-principles prediction of a high-pressure hydrous phase of AlOOH. Phys Rev B 83:054115. https://doi.org/10.1103/PhysRevB.83.054115
Verma AK, Modak P, Stixrude L (2018) New high-pressure phases in MOOH (M═Al, Ga, In). Am Miner 103:1906–1917. https://doi.org/10.2138/am-2018-6634
Xu W, Greenberg E, Rozenberg G, Pasternak MP, Bykova E, Boffa-Ballaran T, Dubrovinsky L, Prakapenka V, Hanfland M, Vekilova OY, Simak SI, Abrikosov I (2013) Pressure-induced hydrogen bond symmetrization in iron oxyhydroxide. Phys Rev Lett 111:175501. https://doi.org/10.1103/PhysRevLett.111.175501
Xu C, Nishi M, Inoue T (2019) Solubility behavior of δ-AlOOH and ϵ-FeOOH at high pressures. Am Miner 104:1416. https://doi.org/10.2138/am-2019-7064
Zhang JS, Hao M, Ren Z, Chen B (2019) The extreme acoustic anisotropy and fast sound velocities of cubic high-pressure ice polymorphs at mbar pressure. Appl Phys Lett 114:191903. https://doi.org/10.1063/15096989

Publisher's Note